



## Applied Surface Science

journal homepage: [www.elsevier.com/locate/apsusc](http://www.elsevier.com/locate/apsusc)

## Effect of surface area of substrates aiming the optimization of carbon nanotube production from ferrocene

A.G. Osorio\*, C.P. Bergmann

Laboratory of Ceramics Materials, LACER, Department of Materials, Federal University of Rio Grande do Sul, Brazil

## ARTICLE INFO

## Article history:

Received 7 August 2012

Received in revised form

24 September 2012

Accepted 23 October 2012

Available online 1 November 2012

## Keywords:

Synthesis

Carbon nanotubes

Ferrocene

Surface area

## ABSTRACT

Ferrocene is widely used for the synthesis of carbon nanotubes due to its ability to act as catalyst and precursor of the synthesis. This paper proposes an optimization of the synthesis of carbon nanotubes from ferrocene, using a substrate with high surface area for their nucleation. Four different surface areas of silica powder were tested: 0.5, 50, 200 and 300 m<sup>2</sup>/g. Raman spectroscopy and microscopy were used to characterize the product obtained and X-ray diffraction and thermal analysis were also performed to evaluate the phases of the material. It was observed that the silica powder with the highest surface area allowed the synthesis of carbon nanotubes to occur at a lower temperature (600 °C), whereas substrates with a surface area lower than 50 m<sup>2</sup>/g will only form carbon nanotubes at temperatures higher than 750 °C. In order to evaluate the influence of chemical composition of the substrate, three different ceramic powders were analyzed: alumina, silica and zirconia. carbon black and previously synthesized carbon nanotubes were also used as substrate for the synthesis and the results showed that the chemical composition of the substrate does not play a relevant role in the synthesis of carbon nanotubes, only the surface area showed an influence.

© 2012 Elsevier B.V. All rights reserved.

## 1. Introduction

Although carbon nanotubes (henceforth to be called CNTs) have been widely studied and produced all over the world, industry is still searching for a feasible route to grow this material that does not require high temperatures and expensive precursors. Ferrocene (Fe(C<sub>5</sub>H<sub>5</sub>)<sub>2</sub>) is an organometallic compound consisting of two cyclopentadienyl rings bonded by an iron atom. This structure is also known as a sandwich compound and it is being used as an alternative to produce feasible CNTs because of its ability to serve as both precursor and catalyst of the synthesis [1–3]. In addition, another major advantage of ferrocene is the absence of expensive and hazardous precursors to produce CNTs. Ferrocene has a melting point of 173 °C and a boiling temperature of 249 °C. These properties allow the decomposition of ferrocene to occur at a relatively low temperature. This feature allows the ferrocene to decompose at a very fast rate when a higher temperature is used. Some authors [4–6] managed to design a reactor where a solution containing ferrocene is fed continuously, providing a continuous production. Although these techniques have considerably improved the

efficiency of CNT synthesis, the main problem with this route is that these nanotubes tend to deposit/attach to the walls of the tube reactor and their removal from the tube is rather difficult, which leads to a low production efficiency. In addition, the synthesis temperature is still reasonably high [1,6–9]. This study proposes for the first time a synthesis route where ceramic nanopowders are used as substrate for the deposition and growth of CNTs using ferrocene alone as catalyst and precursor. This route allows the use of lower temperatures as well as the absence of hazardous gases as precursors. Moreover, one observed that the use of high surface area nanopowders as substrate provide a higher efficiency in the production and removal of CNTs from the reactor, since all nanotubes are synthesized on these particles, which are then easily removed from the tube reactor.

The following paper presents the results obtained for the nucleation and growth of CNTs when different surface areas of silica nanopowders are used as substrates. Powders of different chemical compositions as support to grow CNTs were also tested in order to evaluate the influence of the chemical composition on the growth of CNTs. The main goal of this paper is to evaluate whether the chemical composition and the surface area of the nanoparticles used as substrate play an important role in the synthesis and growth of CNTs through the Chemical vapor deposition (CVD) technique, using ferrocene as both carbon source and catalyst for the nucleation and growth of nanotubes.

\* Corresponding author at: Av. Osvaldo Aranha, 99, sala 705C, Zipcode 90035-190, Porto Alegre (RS), Brazil. Tel.: +55 51 33083637; fax: +55 51 33083405.

E-mail address: [osorio.alice@gmail.com](mailto:osorio.alice@gmail.com) (A.G. Osorio).

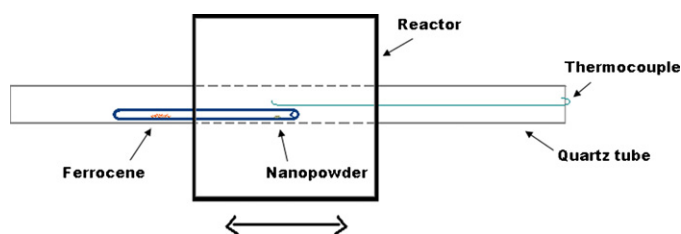


Fig. 1. Illustration of the tube reactor.

## 2. Material and methods

Three different ceramic powders were evaluated as the substrate for the nucleation of CNTs: alumina ( $\text{Al}_2\text{O}_3$ ), silica ( $\text{SiO}_2$ ) and zirconia ( $\text{ZrO}_2$ ). Alumina was purchased from Sigma–Aldrich, and silica and zirconia were supplied by Evonik Industries. Carbon black was also tested as a substrate; this material was provided by cabot industry. Four different surface areas of silica powder were tested: 0.5, 50, 200 and  $300\text{ m}^2/\text{g}$ . These nanopowders were also supplied by Evonik Industries (Aerosil OX50, 200 and 300), except for  $0.5\text{ m}^2/\text{g}$  silica, which was obtained from milling commercial quartz supplied by the mining industry *Mineração Lopus Ltda*. Ferrocene was purchased from Sigma–Aldrich.

The CVD apparatus built for the experiments is basically composed of a 30 mm inner diameter quartz glass tube placed into a cylindrical furnace that can slide along the tube (Illustration in Fig. 1). Inert gas is pumped into the tube in order to guarantee that no oxidation will occur during the growth of nanotubes. The gas used was highly pure helium gas at 300 sccm ( $5 \times 10^{-6}\text{ m}^3/\text{s}$ ). A thermocouple was placed into the quartz tube, where the reaction occurs, and independent temperature controllers were attached to the reactor.

For the synthesis of CNTs on different powders, 0.1 g of ferrocene is placed inside a smaller quartz tube that acts as a crucible. Half of this crucible is placed outside and half inside the furnace. The part of the crucible outside the furnace is where the ferrocene is placed, and 0.0025 g of nanopowder is placed at the half of the crucible inside the furnace (Fig. 1). The temperature is set to increase until it reaches the temperature required. Subsequently, the oven is heated at  $30^\circ\text{C}/\text{min}$  rate and once the required temperature is reached, the furnace slides over the ferrocene powder, which undergoes pyrolysis with nucleation and growth of CNTs, therefore, occurring in a couple of minutes. The authors propose that the carbon and iron elements decomposed from ferrocene are dragged along the quartz tube by the helium gas until they reach the nanopowder with a high surface area, where nucleation and growth of CNTs takes place. At the end of the synthesis, a black powder is obtained where the nanopowder was placed and nearly no remaining material is observed on the tube walls.

The product of the synthesis was evaluated regarding its structure with a Raman spectroscope, model Renishaw inVia Spectrometer System. The experiments were performed at room temperature, at a range of  $0\text{--}3100\text{ cm}^{-1}$  using a laser of  $514\text{ nm}$ . Scanning and transmission electron microscopy (SEM and TEM) were also performed to characterize the morphology of the nanotubes and nanoparticles. A SEM model Jeol JSM 6060 was, therefore, used to characterize these materials, and a TEM Jeol JEM 1200ExII. In order to measure the surface area of all powders,  $\text{N}_2$  adsorption–desorption isotherm measurements were carried out at  $77\text{ K}$  using an ASAP 2020 apparatus, at a relative pressure ( $P/P_0$ ) from 0 to 0.99.0

Four different surface areas of silica nanopowders were tested ( $0.5$ ,  $50$ ,  $200$  and  $300\text{ m}^2/\text{g}$ ) with the synthesis temperature ranging from  $600$  to  $850^\circ\text{C}$ . In order to evaluate the influence of chemical composition of the substrates on the nucleation and growth

Table 1

Identification of samples indicating the nanopowder and the surface area of each sample.

Material	Surface area ( $\text{m}^2/\text{g}$ )
$\text{Al}_2\text{O}_3$	170
$\text{ZrO}_2$	40
$\text{SiO}_2$	190
P-CNTs	62
Carbon black	240

of CNTs, three different ceramic nanopowders as support for the growth of CNTs were tested. The codes assigned for each of them as well as their surface area are described in Table 1. In addition, CNTs were also synthesized using previously grown CNTs (P-CNTs) and also using carbon black material (code also shown in Table 1).

For the synthesis of CNTs on different materials as substrates, a temperature of  $750^\circ\text{C}$  was applied in order to guarantee that the nucleation would occur regardless of the surface area of the nanopowder support.

According to recent publications [10–12], iron-containing phases in CNTs synthesized from ferrocene are inherent to the production process. Some authors have achieved CNTs filled with  $\alpha$ -iron,  $\gamma$ -iron and iron carbides [10,13,14]. These phases provide a magnetic response to the nanotubes, which is seen as a potential application in magnetic devices. Therefore, tests of the chemical composition and magnetic properties of the contents were also carried out on the synthesized material in order to evaluate whether the fast route proposed here still guarantees that the CNTs are filled with magnetic material.

The phase composition of the iron trapped in the CNTs was evaluated by X-ray diffraction and thermal studies; the equipment used was a Philips Diffractometer, model X'Pert MPD with a graphite monochromator and fixed anode operated at  $40\text{ kV}$  and  $40\text{ mA}$  using the  $\text{Cu-K}\alpha$  radiation. Thermal studies were carried out using a TGA/SDTA 851e Mettler Toledo analyzer. The specimens were scanned within a temperature range of  $30\text{--}850^\circ\text{C}$  at a ramp rate of  $5^\circ\text{C}/\text{min}$ , under continuous air flow. This technique was carried out to investigate the thermal stability of the nanotubes as well as the chemical composition of the nanoparticles filling the nanotubes. Magnetic characterization was also performed at room temperature, using an alternating gradient-field magnetometer with the magnetic field,  $H$ , of  $\pm 6000\text{ Oe}$ .

## 3. Results and discussion

### 3.1. Evaluation of the surface area of silica nanopowders

Previous experiments have shown that the surface area of a powder support seems to play a relevant role in the synthesis efficiency of CNTs. Hence, a detailed study of the influence of the surface area of the supports on CNT growth, using the ferrocene only route, proved to be necessary.

According to results obtained from the Raman spectrometer and SEM, CNTs nucleate and grow on the surface of the substrate as entangled bundles of nanotubes (Fig. 2a,b). SEM images obtained for CNT bundles on silica Aerosil 200 show an average size of approximately  $15\text{ }\mu\text{m}$  in diameter (Fig. 2a).

Fig. 3 shows the Raman spectra obtained for the synthesis process applied for each silica surface area, at a temperature range from  $600$  to  $850^\circ\text{C}$  (Because of the temperature gradients present in the reactor tube, the given temperatures are average values).

The presence of CNTs was evidenced in most syntheses performed. This evidence can be seen on the Raman spectra in Fig. 3. In the high-frequency region of the spectrum, the two bands characteristics of carbon nanotubes are observed; these bands indicate the graphite peak (G-band) at about  $1600\text{ cm}^{-1}$ , and the disorder and

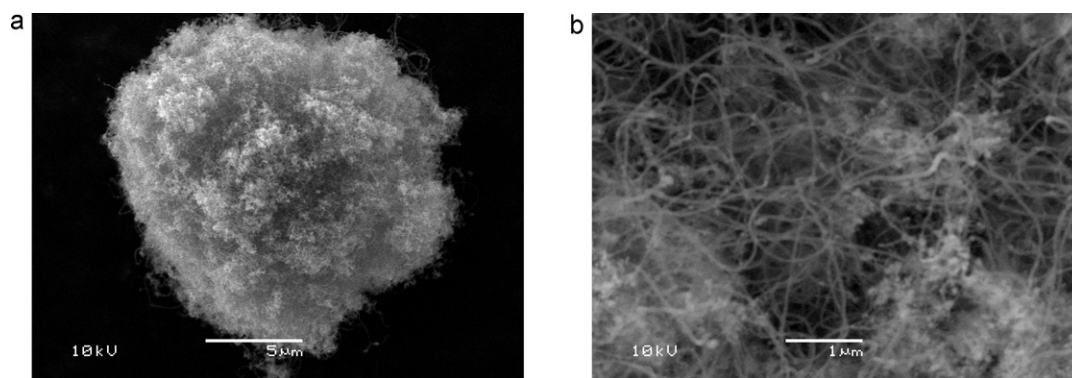


Fig. 2. CNT grown on silica Aerosil200 particles (a); detail of entangled CNTs (b).

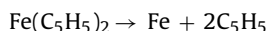
defects of the structure, named D-band, at about  $1380\text{ cm}^{-1}$ . For isolated single-wall CNTs the D-band can be decomposed into two bands whose separation depends on the incident laser energy. A G'-band related to the graphitic structure is also observed at higher frequencies. In the low-frequency part of the spectrum, there is a second region characteristic of CNTs, this region is named Radial breathing mode (RBM). This region at  $100\text{--}300\text{ cm}^{-1}$  is very visible for CNTs that present diameter sizes lower than  $2\text{ nm}$  [15,16]. Bands on the RBM region may not exist in cases where the diameter size of the nanotube is higher than  $2\text{ nm}$ .

Based on the results obtained in these experiments, one can observe that the CNTs synthesized by the proposed route tend to have a diameter size higher than  $2\text{ nm}$  because of the absence of the RBM band. This implies that the nanotubes synthesized here are multi-wall CNTs. Analyzing the images obtained by SEM and Transmission electron microscopy (not shown), and comparing these with the results obtained from the Raman spectrum, one can conclude that CNT growth using this route tends to present a mixture of single and multi-wall CNTs as well as a large variety in length. Nevertheless, the length of the CNTs produced by this route cannot be estimated due to the bundle-like nature in which these nanotubes tend to grow.

The Raman spectra of the final product synthesized with silica Aerosil OX50 at  $600^\circ\text{C}$ , silica commercial quartz at  $600$  and  $650^\circ\text{C}$ , and the synthesis without support from  $600$  to  $700^\circ\text{C}$  are not shown because there was no formation of any material for these temperatures and surface areas.

Evaluating the Raman spectra obtained, one can observe that the silica powder with the highest surface area allows the synthesis of CNTs at the lowest temperatures (Fig. 3a –  $600^\circ\text{C}$ ). When the surface area is decreased to  $200\text{ m}^2/\text{g}$  (Fig. 3b) one can notice that the Raman spectrum for the synthesis at  $600^\circ\text{C}$  does not indicate all characteristic peaks of CNTs, which leads to the conclusion that amorphous carbon is present. For surface areas lower than  $50\text{ m}^2/\text{g}$ , the temperatures at which CNTs can be expected are above  $750^\circ\text{C}$ , below this temperature amorphous carbon is observed. One can also observe that even for the synthesis of CNTs without any support, a minimum synthesis temperature of  $750^\circ\text{C}$  is required. Fig. 4 summarizes the temperatures where CNTs are obtained, according to the surface area of the supports.

Based on the literature [17], ferrocene decomposes as follows:



This implies that at a temperature higher than the boiling point, solid or liquid-like Fe particles and different kinds of hydrocarbons exist in the reaction zone of the CVD equipment.

Thermodynamically, Fe atoms are not expected to react with the quartz material at the temperatures tested. The reason why iron atoms deposit onto the quartz tube are yet to be explained. Based

on the tests performed, we suggest that this occurs simply due to the physical barrier that the quartz tube presents to the iron atoms when they have decomposed and are being carried away by the gas flow, since no reaction between quartz and iron is expected nor observed. Given that iron atoms are heavier, they tend to deposit earlier than the carbon from hydrocarbons on the tube walls by physical adsorption and, thereafter, iron atoms become the catalyst for carbon deposition, as expected. Carbon atoms diffuse into the metal catalyst particles forming iron carbides. Once the nanoparticles of iron carbide are saturated, carbon nanotubes start to grow [16,18,19].

When silica powder is placed inside the tube, one could notice that the powder played the role of a support for the catalyst deposition and nucleation of CNTs. CNTs grow on the silica powder instead of on the tube walls. Based on the results obtained, we suggest that the reaction occurs preferentially on the nanopowder simply due to the higher surface area of the powder when compared to the surface area of the quartz tube. The high surface area also allows the iron adsorption to occur at a lower temperature. In addition, the iron atoms deposited via ferrocene pyrolysis tend to present a higher surface area when compared to iron films used in different synthesis routes [20,21]. A high surface area allows the carbon atoms to diffuse quickly to the metal catalyst particles [18]. This could explain the fast nucleation and growth of CNTs.

Studies performed on the final product of the reaction using Raman spectroscopy, EDS-SEM, TEM, X-ray diffraction and TGA techniques, showed that the silica powder remains as silica powder whereas iron is found in its metallic and carbide form. This phenomenon is discussed in more detail below.

### 3.2. Phase composition of CNTs

The X-ray diffractogram of samples containing CNTs synthesized by the ferrocene route supported by a powder substrate showed the presence of cementite ( $\text{Fe}_3\text{C}$ ), some metallic iron and graphite phases, as expected (Fig. 5).

The presence of cementite and metallic iron in the samples proves that the route proposed to synthesize CNTs maintains those characteristics of the CNTs that are grown through the ferrocene route, with iron-content phases filling the nanotubes.

In order to guarantee that the CNTs are filled with iron-based phases, a TGA analysis was also performed and the results show a gain in mass at about  $400^\circ\text{C}$  followed by a weight loss of approximately 50%. The weight gain can be attributed to the oxidation of metallic iron; once the temperature reaches  $400^\circ\text{C}$  carbon starts to decompose from the tube walls and the weight loss is pronounced (Fig. 6).

After the thermal analysis, an amount of approximately 50 wt% of the initial material remained on the sample holder. The

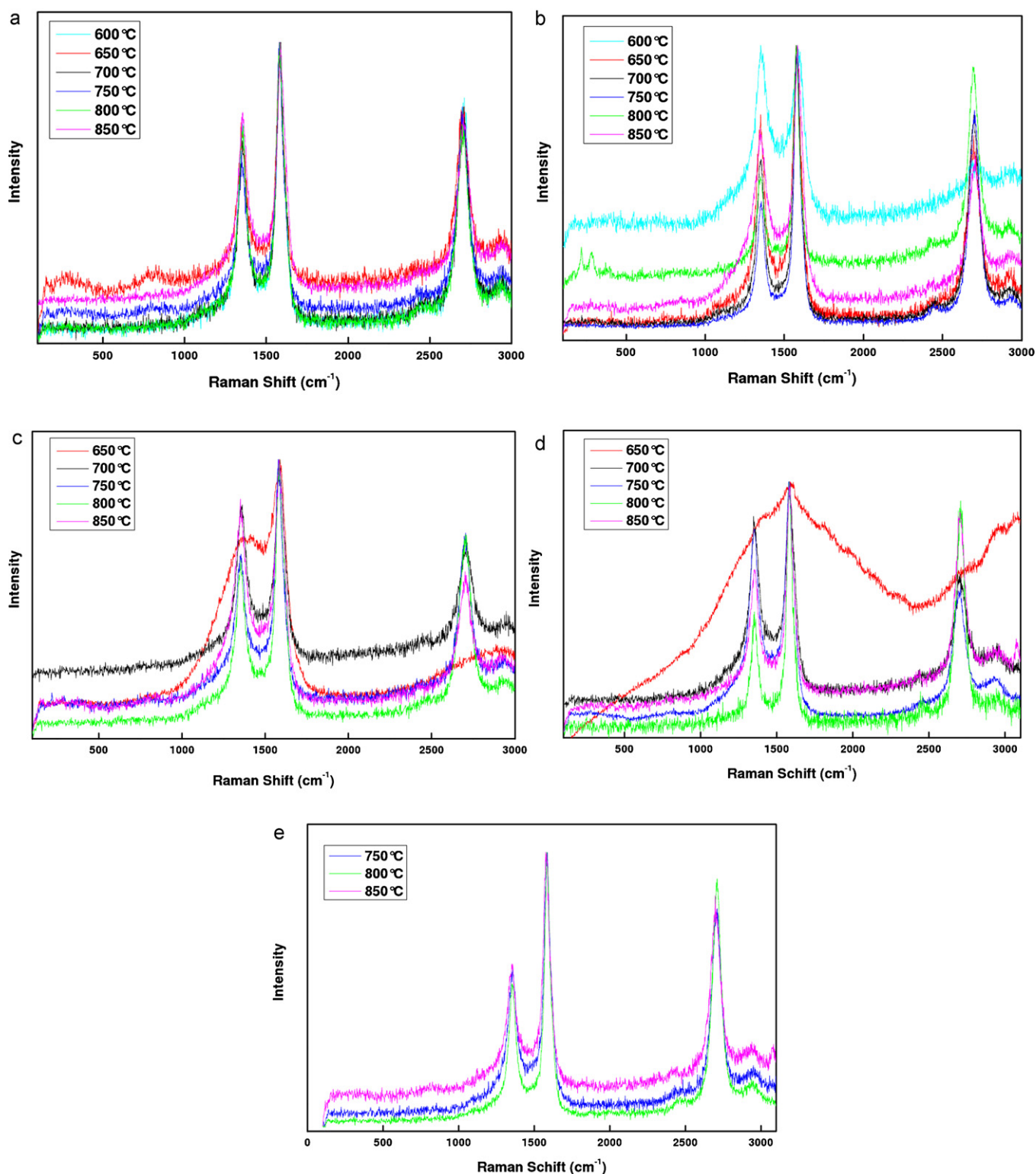


**Fig. 3.** Raman spectra obtained for (a) Aerosil 300, (b) Aerosil 200, (c) Aerosil OX50, (d) commercial quartz and (e) without silica support, at a temperature range of 600–850 °C.

remaining material was analyzed by Raman spectroscopy and indicated iron oxide as hematite (not shown), proving the presence of iron-phase contents in the CNTs.

Magnetization curves of samples synthesized by the ferrocene route for different surface area powder substrates were performed and one could see (not shown) that the CNTs produced by the proposed route were filled with iron-based phases and presented a magnetic response. High coercivities have been obtained from the

materials produced (430–1300 Oe) [22,23]. The samples tested display wide hysteresis loops, showing a coercivity of approximately 660 Oe, a strongly enhanced value when compared to the coercivity value of bulk Fe (0.9 Oe) [24].

In order to analyze whether silica powder is only used as a support for the Fe catalyst, this powder was evaluated to see whether the silica powder maintains its initial formulae altogether with the CNTs, after the synthesis. The X-ray Diffractogram does not show



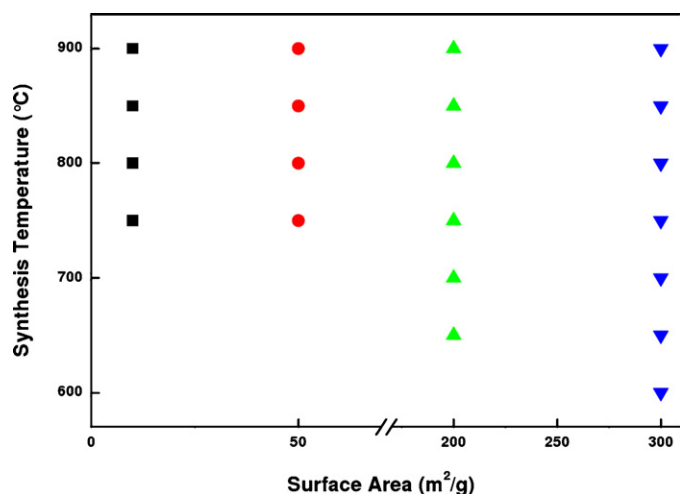


Fig. 4. Summary of results indicating in which temperature CNTs are synthesized, according to the surface area of the supports.

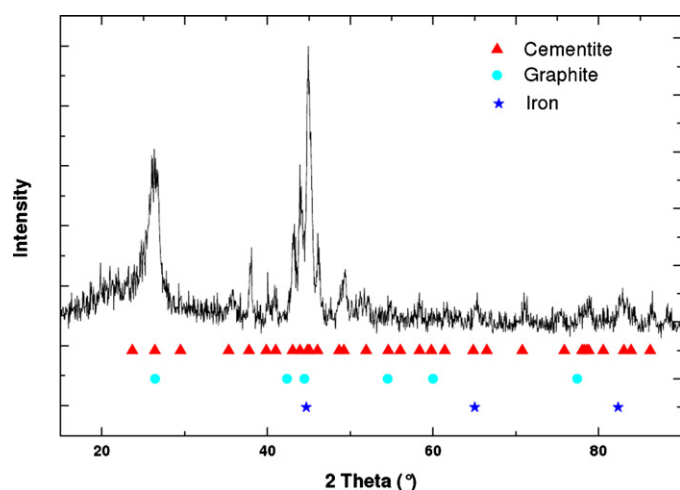


Fig. 5. DRX diffractogram of CNTs synthesized by the ferrocene route.

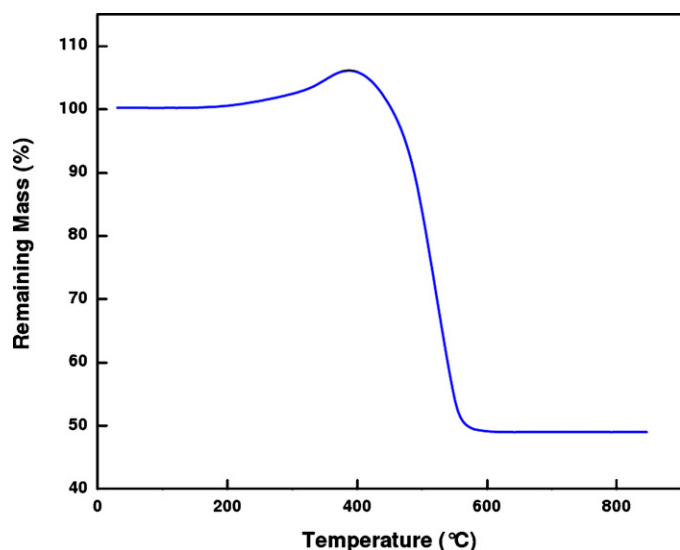


Fig. 6. TGA thermogram obtained for CNTs filled with iron content phases.



Fig. 7. TEM image showing a CNT filled with iron-based material (dark spots inside the nanotube) and a silica nanoparticle (light-gray round particle).

the presence of silica since its amount is very low in comparison to the amount of iron-based contents and nanotubes. Therefore, EDS–SEM (Energy dispersive X-ray spectrometer attached to a SEM) was performed and silica nanoparticles were spotted on the screen. The TEM image shown in Fig. 7 illustrates the presence of the silica nanopowder after the reaction of synthesis.

### 3.3. Evaluation of the chemical composition of the substrates

Different ceramic powders were also used as substrate for the nucleation and growth of CNTs in order to evaluate whether chemical composition of the support plays a relevant role in CNT synthesis. The presence of CNTs was observed on all ceramic substrates tested (alumina, silica and zirconia) when the synthesis was performed at 750 °C. This evidence can be seen on the Raman spectrum in Fig. 8. All bands characteristic of CNTs are, therefore, observed on the Raman spectrum.

Temperatures ranging from 600 to 850 °C were also tested on alumina and zirconia nanopowders, and one could observe that CNTs only grew at 750 °C for zirconia and at 650 °C for alumina. These results are in accordance with previous studies performed for silica nanopowders with different surface areas. Since the surface area of zirconia powder is 40 m<sup>2</sup>/g, it was expected that it would only nucleate CNTs at temperatures higher than 750 °C whereas the alumina powder was expected to nucleate at lower temperatures, since its surface area is much larger than zirconia powder.

Based upon the study performed so far on the synthesis of CNTs using the ferrocene route with nanopowders as supports, one can state that the chemical composition of the substrate does not play an important role in the synthesis of CNTs, since only the surface area is relevant. This conclusion contradicts previous papers [25,26] that consider the substrate composition an important issue. According to the present work, the only concern to produce CNTs using this route, is to choose a substrate resistant to iron diffusion at the synthesis temperature. It is important to highlight

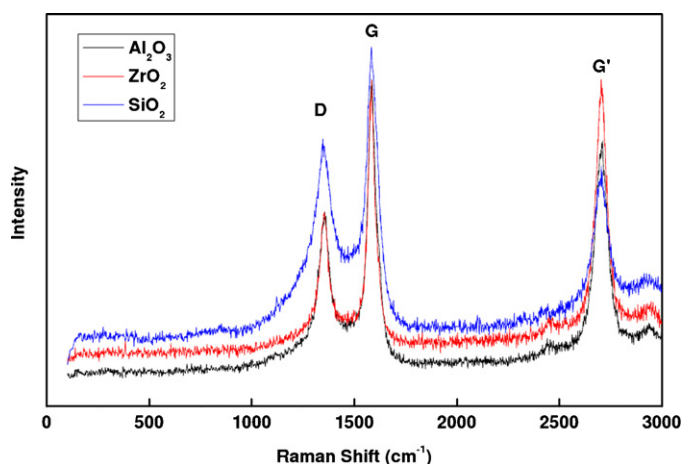


Fig. 8. Raman spectrum of nanotube synthesized onto nanopowder supports at 750 °C.

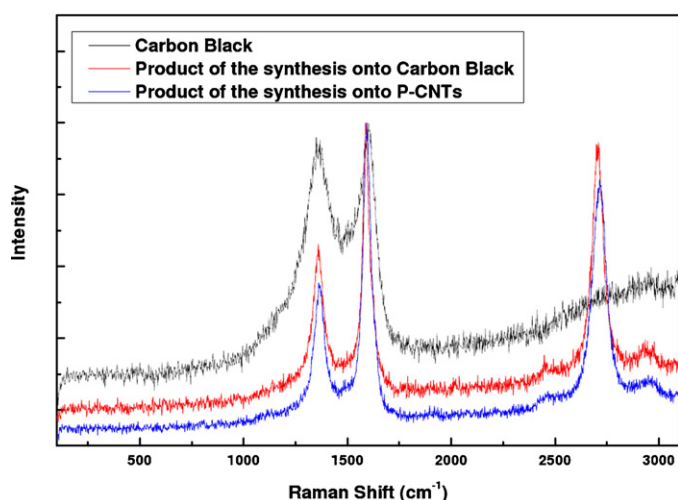


Fig. 9. Raman spectrum of CNTs synthesized onto P-CNTs and carbon black material.

that CNTs grown from iron films as catalyst are not synthesized using ferrocene, they use hydrocarbon gases as precursors.

In order to sustain the conclusion that the surface area is the major issue that governs the adsorption of iron atoms and, consequently, the nucleation and growth of CNTs, the ferrocene route was also performed using P-CNTs and carbon black material as substrate/support for the Fe catalyst. Subsequently, one could observe that CNTs were produced on these supports (Fig. 9). Fig. 9 shows the Raman spectra of carbon black before and after the synthesis of CNTs. One can notice that before the synthesis, only amorphous carbon can be spotted, whereas after the synthesis only CNTs are seen. The carbon black powder is still present among the CNTs after the synthesis. However, due to its diminished amount, it cannot be observed on the Raman spectrum.

One can observe that the chemical composition of the support for Fe atoms deposition does not have any influence on the reaction, since the reaction occurred at the expected temperature, considering the surface area of each tested nanopowder. The final product obtained for all syntheses were CNTs filled with iron-based material and no evidence of any other material and/or reaction was seen. Thus, based on the studies performed in this work, the authors came to the conclusion that the physical adsorption of iron onto the support is exclusively related to the physical barrier that a high surface area material implies.

#### 4. Conclusion

This paper presents an optimized process for the production of CNTs by means of CVD where ferrocene is decomposed, acting as a floating catalyst and precursor. High surface area powders are used as substrate to optimize the temperature of synthesis and for the removal of CNTs from the tube reactor. Iron nanoparticles are physically adsorbed on the nanopowder surface and the carbon atoms are, therefore, diffused into the iron, providing the necessary environment to grow CNTs.

CNTs grow on the nanopowder support, rather than on the reactor walls, due to a higher physical barrier provided by the higher surface area of the powder supports. This feature facilitates a continuous withdrawal of CNTs from the reactor, making it suitable for large-scale production. In addition, the authors also concluded that the higher the surface area of the supports, the lower the synthesis temperature of CNTs.

The chemical composition of the support does not have any influence on the nucleation and growth of CNTs via the ferrocene route and the proposed route maintained all the previously seen and expected characteristics of the CNTs.

#### Acknowledgments

The authors would like to acknowledge the Center of Electronic Microscopy (CME) of the Federal University of Rio Grande do Sul for permitting the use of their microscopes. The authors would also like to thank Evonik Industries for the powders provided.

#### References

- [1] R. Bhatia, V. Prasad, Synthesis of multiwall carbon nanotubes by chemical vapor deposition of ferrocene alone, *Solid State Communications* 150 (2010) 311–315.
- [2] K. Kuwana, K. Saito, Modeling CVD synthesis of carbon nanotubes: nanoparticle formation from ferrocene, *Carbon* 43 (2005) 2088–2095.
- [3] K.P.S.S. Hembram, Mohan G. Rao, Structural and surface features of multiwall carbon nanotube, *Applied Surface Science* 257 (2011) 5503–5550.
- [4] M. Terrones, H. Terrones, N. Grobert, W.K. Hsu, Y.Q. Zhu, J.P. Hare, H.W. Kroto, D.R.M. Walton, P. Kohler-Redlich, M. Rühle, J.P. Zhang, A.K. Cheetham, Efficient route to large arrays of CNx nanofibers by pyrolysis of ferrocene/melamine mixtures, *Applied Physics Letters* 75 (25) (1999) 3932.
- [5] R.M.M. Abbaslou, J. Soltan, A.K. Dalai, The effects of carbon concentration in the precursor gas on the quality and quantity of carbon nanotubes synthesized by CVD method, *Applied Catalysis A: General* 372 (2010) 147–152.
- [6] D. Conroy, A. Moisala, S. Cardoso, A. Windle, J. Davidson, Carbon nanotube reactor: ferrocene decomposition, iron particle growth, nanotube aggregation and scale-up, *Chemical Engineering Science* 65 (2010) 2965–2977.
- [7] A. Moisala, A.G. Nasibulin, D.P. Brown, H. Jiang, L. Khriachtchev, E.I. Kauppinen, Single-walled carbon nanotube synthesis using ferrocene and iron pentacarbonyl in a laminar flow reactor, *Chemical Engineering Science* 61 (2006) 4393–4402.
- [8] Y.T. Lee, N.S. Kim, J. Park, J.B. Han, Y.S. Choi, H. Ryu, H.J. Lee, Temperature-dependent growth of carbon nanotubes by pyrolysis of ferrocene and acetylene in the range between 700 and 1000 °C, *Chemical Physics Letters* 372 (2003) 853–859.
- [9] S. Maghssoodi, A. Khodadadi, Y. Mortazavi, A novel continuous process for synthesis of carbon nanotubes using iron floating catalyst and MgO particles for CVD of methane in a fluidized bed reactor, *Applied Surface Science* 256 (2010) 2769–2774.
- [10] E.F. Antunes, V.G. de Resende, U.A. Mengui, J.B.M. Cunha, E.J. Corat, M. Massi, Analyses of residual iron in carbon nanotubes produced by camphor/ferrocene pyrolysis and purified by high temperature annealing, *Applied Surface Science* 257 (2011) 8038–8043.
- [11] F.C. Dillon, A. Bajpai, A. Koós, S. Downes, Z. Aslam, N. Grobert, Tuning the magnetic properties of iron-filled carbon nanotubes, *Carbon* (2012), <http://dx.doi.org/10.1016/j.carbon.2012.03.040>.
- [12] A. Nagata, H. Sato, Y. Matsui, T. Kaneko, Y. Fujiwara, Magnetic properties of carbon nanotubes filled with ferromagnetic metals, *Vacuum* (2012) 008, <http://dx.doi.org/10.1016/j.vacuum.2012.03>.
- [13] E. Park, J. Zhang, S. Thomson, O. Ostrovski, R. Howe, Characterization of phases formed in the iron carbide process by X-ray diffraction, Mössbauer, X-ray

- photoelectron spectroscopy, and Raman spectroscopy analyses, Metallurgical and Materials Transactions B 32B (2001) 839.
- [14] V.G. de Resende, A. Peigney, E. de Grave, C. Laurent, *In situ* high-temperature Mössbauer spectroscopic study of carbon nanotube–Fe–Al<sub>2</sub>O<sub>3</sub> nanocomposite powder, *Thermochimica Acta* 494 (2009) 86–93.
- [15] E. Flahaut, C. Laurent, A. Peigney, Catalytic CVD synthesis of double and triple-walled carbon nanotubes by the control of the catalyst preparation, *Carbon* 43 (2005) 375–383.
- [16] J.H. Lehman, M. Terrones, E. Mansfield, K.E. Hurst, V. Meunier, Evaluating the characteristics of multiwall carbon nanotubes, *Carbon* 49 (2011) 2581–2602.
- [17] K. Kuwana, K. Saito, Modeling ferrocene reactions and iron nanoparticle formation: application to CVD synthesis of carbon nanotubes, *Proceedings of the Combustion Institute* 31 (2007) 1857–1864.
- [18] F. Danafar, A. Fakhru'l-Razi, M.A.M. Salleh, D.R.A. Biak, Fluidized bed catalytic chemical vapor deposition synthesis of carbon nanotubes—a review, *Chemical Engineering Journal* 155 (2009) 37–48.
- [19] S. Esconjauregui, C.M. Whelan, K. Maex, The reasons why metals catalyze the nucleation and growth of carbon nanotubes and other carbon nanomorphologies, *Carbon* 47 (2009) 659–669.
- [20] A. Gohier, K.-H. Kim, E.D. Norman, L. Gorintin, P. Bondavalli, C.S. Cojocaru, Spray-gun deposition of catalyst for large area and versatile synthesis of carbon nanotubes, *Applied Surface Science* 258 (2012) 6024–6028.
- [21] M.J. Bronikowski, CVD growth of carbon nanotube bundle arrays, *Carbon* 44 (2006) 2822–2832.
- [22] N. Grobert, W.K. Hsu, Y.Q. Zhu, J.P. Hare, H.W. Kroto, D.R.M. Walton, Enhanced magnetic coercivities in Fe nanowires, *Applied Physics Letters* 75 (1999).
- [23] A. Leonhardt, S. Hampel, C. Müller, I. Mönch, R. Koseva, M. Ritschel, D. Elephant, K. Biedermann, B. Büchner, Synthesis, properties, and applications of ferromagnetic-filled carbon nanotubes, *Chemical Vapour Deposition* 12 (2006) 380–387.
- [24] F. Geng, H. Cong (2006) *apud* R.M. Bozorth, *Ferromagnetism*, D. Van Nostrand Company, Inc., Toronto, New York, London, 1951.
- [25] S.K. Pal, S. Kar, S. Lastella, A. Kumar, R. Vajtai, S. Talapatra, T. Borca-Tasciuc, P.M. Ajayan, Importance of Cr<sub>2</sub>O<sub>3</sub> layer for growth of carbon nanotubes on superalloys, *Carbon* 48 (2010) 844–853.
- [26] P. Ciambelli, D. Sannino, M. Sarno, C. Leone, U. Lafont, Effects of alumina phases and process parameters on the multiwalled carbon nanotubes growth, *Diamond & Related Materials* 16 (2007) 1144–1149.